energy&fuels

Article

pubs.acs.org/EF

Detailed Modeling of NO_x and SO_x Formation in Co-combustion of Coal and Biomass with Reduced Kinetics

Xiaolin Wei,*[,†] Xiaofeng Guo,[†] Sen Li,[†] Xiaohai Han,[‡] Uwe Schnell,[§] Günter Scheffknecht,[§] and Benedetto Risio[‡]

[†]Center for Plasma and Combustion Research, Institute of Mechanics, Chinese Academy of Sciences (CAS), Beijing 100190, People's Republic of China

[‡]RECOM Services GmbH, D-70569 Stuttgart, Germany

[§]Institute of Combustion and Power Plant Technology, University of Stuttgart, Pfaffenwaldring 23, D-70569 Stuttgart, Germany

ABSTRACT: In the paper, the numerical simulation program coupled with the detailed chemical reaction mechanism and computational fluid dynamics software was applied to calculate the concentration profiles of CO, NO_x, and SO_x during co-combustion of coal and biomass. The predicted data are compared to experimental results in an entrained flow combustion reactor to validate the numerical method for pulverized coal combustion. The characteristics of pollutant emissions in co-combustion with coal and three typical kinds of biomasses (Swedish wood, Danish straw, and sewage sludge) are also investigated. NO formation is significantly affected by the reactor temperature, and an increasing temperature obviously enhances the NO concentration. In the range of the calculated temperature, the final SO_2 emission level is not obviously influenced by the temperature. Co-combustion technology could effectively reduce the pollutant emissions, and the effect is proportional to the blending ratio of biomass. The biomass with low contents of nitrogen and sulfur and a high volatile content and lower heating value is an ideal co-fired fuel to reduce NO and SO_2 emissions.

1. INTRODUCTION

In pulverized coal combustion, fuel N conversion to NO is generally the major source of NO (>80%), with some contribution from thermal NO.[1,2] During coal devolatilization, fuel N is distributed between the volatiles and the solid char. It is generally assumed in modeling that nitrogen-containing volatiles either consist of or are rapidly converted to HCN and/or NH_3. Subsequently, HCN and/or NH_3 are oxidized to NO via the homogeneous reactions involving the radicals (O, H, OH, and HO_2), while they are competitively reduced to N_2. The conversion of nitrogen-containing char occurs via the heterogeneous reactions involving the solid char, which also result in the formation of NO (by oxidation) or N_2 (by reduction).

During solid fuel combustion, the NO_x formation is influenced by several factors, e.g., temperature, equivalence ratio, mixing, residence time, etc. Traditional global mechanisms are sometimes not able to simulate the process over an adequate range with desired accuracy. On the other hand, a number of comprehensive detailed mechanisms describing hydrocarbon combustion and the related N chemistry have been developed.[3−5] The direct use of these mechanisms in computational fluid dynamics (CFD) modeling of practical problems, however, is usually very expensive or even impossible, owing to the extremely large computing time and costs. Reasonably reduced kinetics based on these mechanisms can retain the important features of the original mechanisms and also greatly reduce the computing time. Reduced schemes in the CFD modeling of NO_x formation in coal combustion have been reported.[6,7,9−12]

On the basis of the previous work,[6] Xu et al. postulated a simpler 4 steps, 8 species reduced mechanism for the prediction of nitric oxide concentrations for advanced reburning, i.e., the hybrid reburning/selective noncatalytic reduction (SNCR).[7] A systematic reduction method[8] was used to derive the reduced mechanism, including the selection of the full mechanism, the development of the skeletal mechanism, and the selection of steady-state species. The reduced mechanism was derived from a 62 steps, 20 species skeletal mechanism,[6] which itself was based on a 312 steps, 50 species full mechanism. The 4 step integrated submodel for advanced reburning has been combined with a comprehensive CFD combustion code, PCGC-3. The predicted average axial NO concentration with advanced reburning (NH_3 injection) followed experimental trends.[9]

Han et al. developed a 12 steps, 16 species reduced mechanism for the conditions of CH_4 reburning in the coal-fired furnace.[10] The reduced mechanism was derived from a 137 steps, 43 species skeletal mechanism, which was based on the "GRI 3.0" mechanism with 325 steps, 53 species.[5] The reduced mechanism is then integrated into the three-dimensional (3D) combustion simulation CFD program "AIOLOS". The simulation results agree well with the experimental data for CH_4 reburning during pulverized coal combustion. Further, Han et al. developed a 10 steps, 14 species reduced mechanism for advanced reburning.[11] The reduced mechanism was derived from a 105 steps, 39 species skeletal mechanism, which was based on the "GADM98" mechanism with 438 steps, 64

Special Issue: 7th International Symposium on Coal Combustion

Received: November 6, 2011
Revised: December 24, 2011
Published: December 26, 2011

   dx.doi.org/10.1021/ef201729r | *Energy Fuels* 2012, 26, 3117−3124

species.[4] CFD simulations were performed with the reduced kinetics for pure reburning and hybrid reburn/SNCR in a coal-fired reactor. The comprehensive modeling gave quite satisfactory results for wide ranges of the parameters.

Lv et al.[12] developed a joint mechanism including 44 species and 150 elementary reactions based on the mechanism by Rota et al.[13] and the scheme by Zebetta et al.[14] to predict the hybrid NO_x control process. The simplification employed related graphs and the rate-of-product method and was validated by comparing to reported experimental data. To handle CFD simulation of practical problems, a reduced mechanism was accordingly established including 18 global steps and 22 species and was tested by comparing its predicted results to those of the joint mechanism. Perfect coherency between them is observed at different operating conditions, and the deviation is negligible compared to the general measuring uncertainty.

In the paper, on the basis of the previous work,[10,11] a reduced mechanism involving NO_x and SO_x reaction kinetics was applied to predict the concentration profiles of CO, NO_x, and SO_x during pulverized coal combustion. The effect of the combustion temperature on NO and SO_2 formation is analyzed. The characteristics of pollutant emissions in co-combustion with coal and three typical kinds of biomasses (Swedish wood, Danish straw, and sewage sludge) at different blending ratios and temperatures are investigated.

2. NUMERICAL SIMULATION METHOD

The detailed modeling method of NO_x formation in pulverized coal combustion with reduced kinetics has been described in detail elsewhere,[10,11] and in this work, the sulfur chemistry is also integrated into the reduced kinetics. A brief description of the numerical simulation method is given here.

2.1. Reduction of the Detailed Mechanism. First, a skeletal mechanism was derived from the full mechanism by eliminating unimportant reaction steps through sensitivity analysis, partial equilibrium analysis, and integral reaction flow analysis.[8,15] Second, the quasi-steady-state (QSS) species are identified from the reactions in the skeletal mechanism, and the reactions including each QSS species are eliminated. Finally, a global reaction mechanism is established, and the global reaction rates are determined by the elementary reaction rates in the skeletal mechanism.

The present work chooses the "GADM98" mechanism[4] as one of the original detailed mechanisms, including NO_x formation and C_1 and C_2 hydrocarbon fuels chemistry. Another original detailed mechanism is taken from the "GKDCB96" mechanism for SO_x formation[16] including 66 reactions and 15 species. There are in total 504 reactions and 79 species in the full reaction mechanism. The reduction procedure is performed in conjunction with the SENKIN code[17] in the CHEMKIN package. After the computation, the mechanism reduction program reads data from the CHEMKIN link file and the SENKIN results file that contain the information on the kinetic mechanism and species concentrations, the rates of production, and the sensitivity coefficient of all species with respect to each reaction. The mechanism reduction is performed through analyzing the SENKIN results by means of the developed program.

The skeletal mechanism is derived from the full reaction mechanism by identifying and eliminating unimportant reaction steps through the analysis regarding the major variables under a particular flame condition of interest.[8,15]

The reaction steps having the normalized first-order sensitivity coefficients along the time of the main reaction stretch smaller than a predefined criterion, in this work, 1−5%, will be eliminated

$$S_{k,i}/\max_i(S_{k,i}) < \delta \tag{1}$$

where $S_{k,i}$ is the sensitivity coefficient of the kth species with respect to the ith reaction. The sensitivity coefficient is defined as

$$S_{k,i} = \frac{\partial[X_k]}{\partial A_i} \tag{2}$$

where X_k is the mole fraction of the kth species and A_i is the pre-exponential factor in the Arrhenius expression for the forward rate constant of the ith reaction [$k_i = A_i T^b \exp(-E_i/RT)$].

In addition, the reaction steps are in partial equilibrium fulfilling the following relation along the time of the main reaction stretch:

$$\frac{|k_{f_i} - k_{r_i}|}{\max(k_{f_i}, k_{r_i})} < \delta \tag{3}$$

where k_f and k_r are the forward and reverse reaction rate constants, respectively, and are also omitted from the skeletal mechanism (δ = 5−10%).

To avoid some important reactions being eliminated from the mechanism, the strategy is that all reactions that have a great relative integral reaction flow are retained in the skeletal mechanism

$$\frac{\int_0^{\Delta t} q_i \mathrm{d}t}{\max_i(\int_0^{\Delta t} q_i \mathrm{d}t)} < \delta \tag{4}$$

where the usual value of the criterion δ equals 1−5%, Δt is the time of the reaction stretch, and q_i is the rate of progress of the ith reaction, which fulfills the following equation:

$$q_i = k_{f_i} \prod_{k=1}^{K} [X_k]^{\nu' ki} - k_{r_i} \prod_{k=1}^{K} [X_k]^{\nu'' ki} \tag{5}$$

where K is the total number of the species, ν'_{ki} is the stoichiometric coefficient of the kth species in the ith forward reaction, and ν''_{ki} is the stoichiometric coefficient of the kth species in the ith reverse reaction.

According to the above method, the skeletal mechanism is derived containing 242 reactions and 63 species.

In the skeletal mechanism, the species fulfilling the following relation along the whole reaction stretch are identified as the QSS species:[8]

$$[X_k]\frac{|\dot{\omega}_k^{\mathrm{p}} - \dot{\omega}_k^{\mathrm{d}}|}{\max(\dot{\omega}_k^{\mathrm{p}}, \dot{\omega}_k^{\mathrm{d}})} < \delta \tag{6}$$

where $\dot{\omega}_k^{\mathrm{p}}$ is the production rate of the kth species and $\dot{\omega}_k^{\mathrm{d}}$ is the destruction rate of the kth species. The usual value of the criterion δ equals 0.1−1%.

After the QSS analysis, 15 species are retained, called non-steady state (or major) species. They are O_2, CO, CO_2, CH_4, C_2H_6, H_2, H_2O, N_2, NH_3, HCN, NO, SO, SO_2, SO_3, and H_2S, which will remain in the reduced global mechanism.

The steady-state assumption for a species leads to the algebraic equation

$$\frac{\mathrm{d}[X_k]}{\mathrm{d}t} = \dot{\omega}_k = \sum_i (\nu''_{ki} - \nu'_{ki}) q_i = 0 \tag{7}$$

between reaction rates. The above equations denote the net production rate of the QSS species. Each of these equations can be used to eliminate a reaction rate (because $q_i = 0$) in the balance equation set for the major species. Principally, the present work selects for each QSS species the least sensitive reaction involving the species. This elimination principle ensures the smallest errors, and the reduced mechanism has lower stiffness.[15] The stoichiometry of the resulting equation system defines the global mechanism between the major species. The rate of each global reaction step can be expressed with the rates of the elementary reactions in the skeletal mechanism. After this eliminating procedure, 10 independent reactions (global reaction scheme) were obtained.

dx.doi.org/10.1021/ef201729r | Energy Fuels 2012, 26, 3117−3124

When eq 7 is used to determine the concentration of the QSS species, an algebraic equation set can be obtained that expresses the concentrations of the QSS species in terms of other species (see eq 5). This set of equations is often coupled nonlinearly among those QSS species. Given the concentrations of the major species, the concentrations of QSS species are determined by solving the equation system iteratively. Finally, a Fortran subroutine is automatically generated for calculating the production rate of the major species according to the reduced mechanism. More details about the reduced mechanism and its discussion can be found in refs 10, 11 and 18.

2.2. Integration into the CFD Code "AIOLOS". The developed reduced kinetics for NO_x and SO_x formation under coal-fired conditions was implemented into the 3D furnace simulation CFD program "AIOLOS" developed by the Institute of Combustion and Power Plant Technology at the University of Stuttgart, which mainly deals with pulverized coal combustion. The code "AIOLOS" is based on a conservative finite-volume formulation, using the SIMPLEC or SIMPLE method for velocity−pressure coupling, the standard $k-\varepsilon$ model, or the differential Reynolds stress model for turbulence.[19] Radiative heat transfer is calculated by either a discrete ordinates method or five other different radiation models. The turbulent gas-phase reactions are calculated with the eddy dissipation concept (EDC) model.[20−23] The EDC is a general concept for treating the interaction between turbulence and chemistry in flames.

After the implementation, all of the homogeneous reactions (gas-phase reactions) are calculated with the reduced mechanism. The heterogeneous reactions, i.e., the pyrolysis and char combustion, the heterogeneous sources of N species, the heterogeneous NO_x reduction by char, etc., are calculated with the available models in AIOLOS (see ref 24). The composition of the pyrolysis product as well as the distribution of coal nitrogen within the pyrolysis products is predicted using the functional-group, depolymerization, vaporization, cross-linking (FG-DVC) model[25] in a pre-processing step.[24] Char nitrogen is assumed to be released as the primary product NH_3 during char burnout. To simulate biomass combustion, a model of evaporation of moisture in biomass is used. For both kinds of fuels, the particle shape is assumed to be spheroidal, the size distribution is given using three typical average diameters and proportions according to experimental measurements, and the parameters for pyrolysis and char burnout are also modified for different fuels based on the formula $k_i = A_i \exp(-E_i/RT)$. The corresponding information is shown in Table 1. The

Table 1. Particle Size Distribution and Kinetic Parameters for Pyrolysis and Char Burnout

	coal		biomass	
particle size distribution	10 μm	40%	15 μm	20%
	25 μm	40%	40 μm	40%
	50 μm	20%	75 μm	40%
Kinetic Parameters for Pyrolysis				
A_i (s^{-1})	1.5×10^5		1.667×10^4	
E_i/R (K)	8900		9500	
Kinetic Parameters for Char Burnout				
A_i (s^{-1})	208		500	
E_i/R (K)	9553		9553	

heterogeneous reduction of NO by soot and char is considered for both coal and biomass with a first-order rate expression as

$$\left(\frac{dn_{NO}}{dt}\right)_i = -A_i \exp(-E_i/RT) X_{NO} S_e \quad (8)$$

where n_{NO} is the mole number of NO in kilomoles, X_{NO} is the mole fraction of NO, and S_e is the available external surface area of soot or char. The corresponding rate parameters are $A_i = 4.47 \times 10^{-7}$ kmol m^{-2} s^{-1} Pa^{-1} and $E_i = 9.65 \times 10^3$ K for soot and $A_i = 4.18 \times 10^{-4}$ kmol m^{-2} s^{-1} Pa^{-1} and $E_i = 1.75 \times 10^4$ K for char.[24]

In the present work, seven additional gas species (NH_3, HCN, NO, SO, SO_2, SO_3, and H_2S) over the eight originally existing gas species in AIOLOS (O_2, CO, CO_2, CH_4, C_2H_6, H_2, H_2O, and N_2) were supplemented into the AIOLOS program. Transport equations for these species are to be solved, and the concentration distribution of the species is obtained.

2.3. Description of the Experiment. Tests and simulations are executed for a 20 kW electrically heated pulverized coal-fired entrained flow reactor (EFR). The reactor is schematically shown in Figure 1.

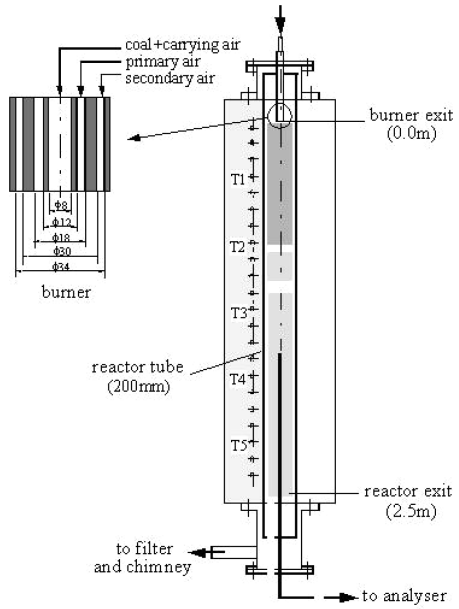

Figure 1. Schematic of the pulverized coal-fired EFR.

The combustion air can be heated to 400 °C. A gravimetric screw conveyor supplies a constant coal-feeding rate between 0.5 and 5 kg/h. The electrically heated reactor has five regulated heating zones with a maximum temperature of 1400 °C, measured by PtRh−Pt thermocouples. The ceramic reactor tube has a length of 2.5 m and an internal diameter of 200 mm. The flue gas composition (NO, NO_2, CO, CO_2, SO_2, and O_2) at different positions is measured online using standard instrumentation [paramagnetism for O_2, non-dispersive infrared (NDIR) for CO and CO_2, chemiluminescence for NO_x, and infrared photometer for SO_2] through a vertically moveable gas probe cooled with oil. The error of the measuring instrument is 1−5 ppmv.

In the present experiment, a German bituminous coal "Göttelborn" is used as a fuel with a feeding rate of 1 kg/h during the tests, and the coal analysis is listed in Table 2. The carrying air with pulverized coal enters the burner center, surrounded by the primary air and the

Table 2. Pulverized Coal and Biomass Analysis Data

	Göttelborn	Swedish wood	Danish straw	sewage sludge
Proximate Analysis (wt %)				
moisture (ar)	1.69	7.80	11.71	5.86
volatile (dry)	31.94	84.10	71.32	48.45
ash (dry)	10.74	0.20	13.42	48.06
fixed carbon (dry)	57.32	15.70	15.26	3.65
LHV (MJ/kg, dry)	30.89	18.52	16.01	10.72
Ultimate Analysis (wt %, dry)				
C	74.16	49.57	41.43	25.77
H	4.42	6.05	4.18	4.31
N	1.18	0.07	1.09	3.02
S	1.12	0.06	0.10	0.81
Cl	0.22	0.01	0.53	0.04
O	8.16	44.04	39.25	17.99

dx.doi.org/10.1021/ef201729r | Energy Fuels 2012, 26, 3117−3124

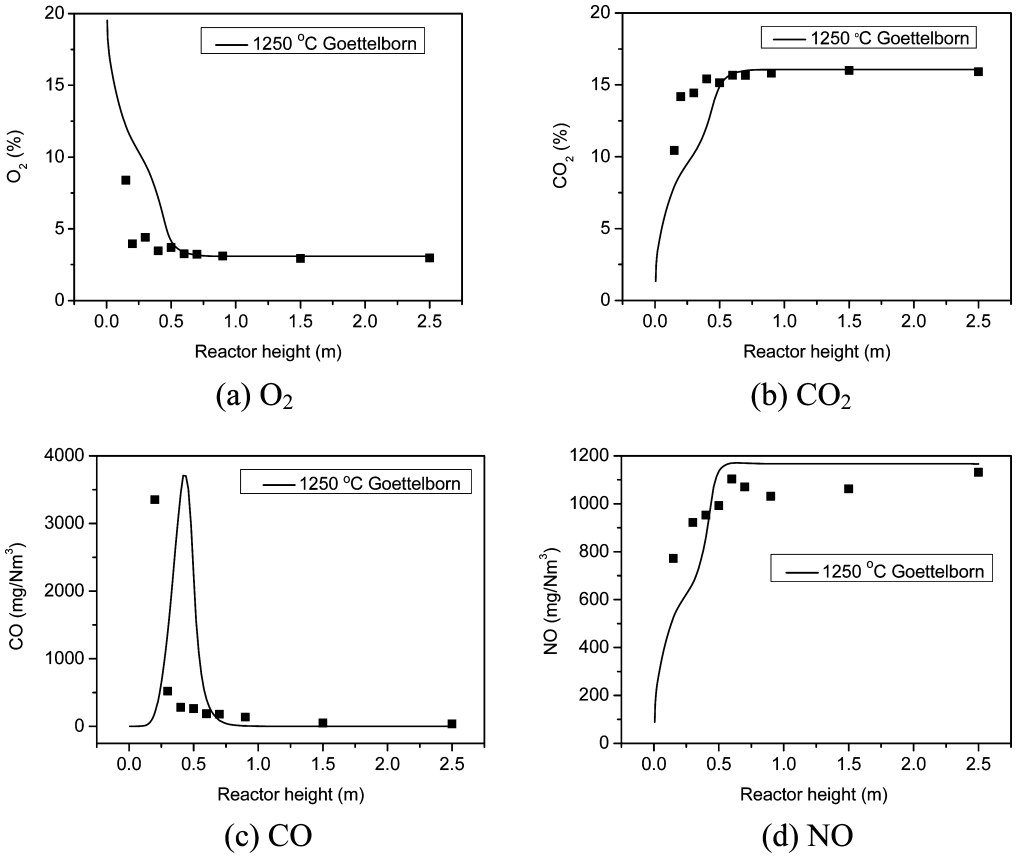

Figure 2. Comparison between the predicted and measured results in EFR (—, predicted result; ■, measured result).

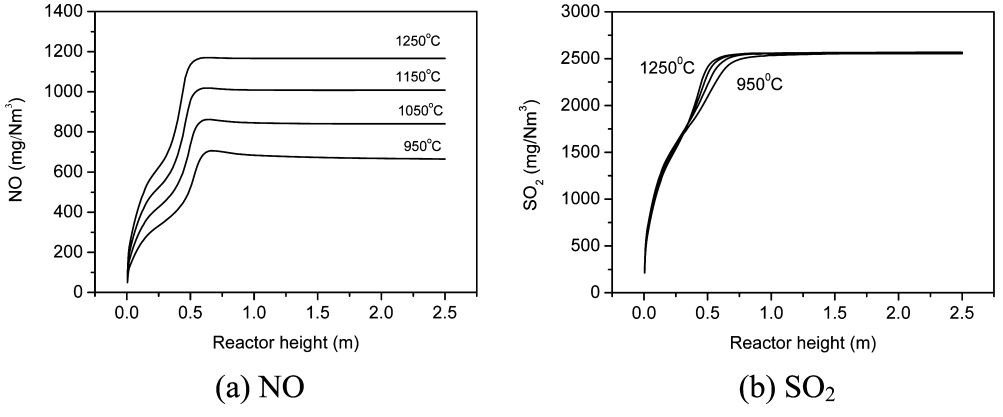

Figure 3. Predicted results of (a) NO and (b) SO_2 concentration distribution for Göttelborn coal along the reactor height for various wall temperatures.

secondary air. The carrying air flux is 1.5 N m^3 h^{-1}. The total flux of the primary and second air is 8 N m^3 h^{-1}, and the ratio between them is 1:2. The air/fuel equivalence ratio λ is 1.15. The wall temperature is 1250 °C.

During the tests, it was found that, besides the controllable parameters, pollutant emissions might be influenced by some unexpected incidents, e.g., a slight variation of fuel composition or a fluctuating feeding rate. For example, the results show that the maximum variation of NO_x under each condition is likely to attain ±20 ppmv. However, the averaged emission during a relatively long time period is obviously close to a constant.[26] Therefore, each experimental data point in this paper is an average result of 2−3 times measurements, with a 2 min interval for one time.

2.4. Model Validation. The predicted data are compared to experimental results in the entrained flow combustion reactor shown in Figure 1 to validate the numerical method. Figure 2 gives the predicted and measured O_2, CO_2, CO, and NO concentration profiles along the reactor height. It can be seen that both results coincide well for the change trend and final emission of various species. However, in the beginning of the coal flame, the predicted concentration of O_2 is higher than the experimental value and the corresponding calculated CO_2 concentration is less than the test data. Also, the predicted CO concentration peak delays to occur, and the calculated NO concentration is lower than the experimental data near the burner. These differences between measured and predicted values might be induced by the ignition delay in the numerical model, or the flow field and coal combustion might be affected by the sampling probe with a relatively big diameter (38 mm) near the burner in the experiments. Nevertheless, the detailed modeling method seems to be able to predict the pulverized coal combustion satisfactorily. For simulating

dx.doi.org/10.1021/ef201729r | Energy Fuels 2012, 26, 3117−3124

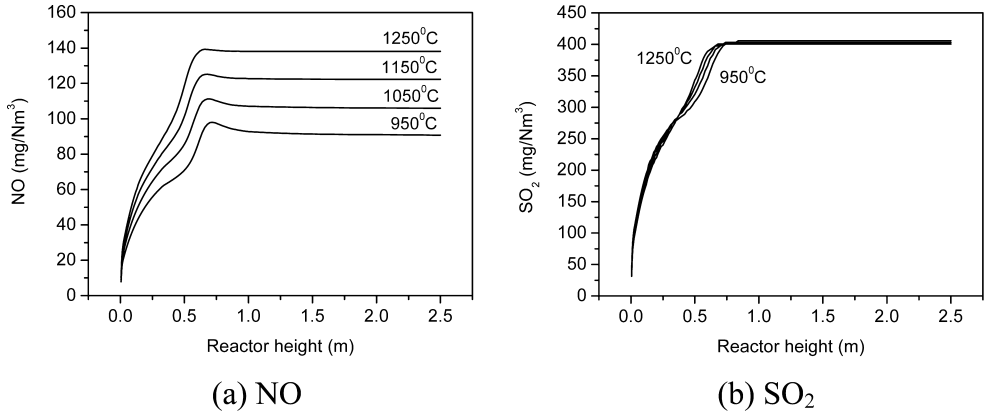

Figure 4. Predicted results of (a) NO and (b) SO_2 concentration distribution for pure Swedish wood along the reactor height for various wall temperatures.

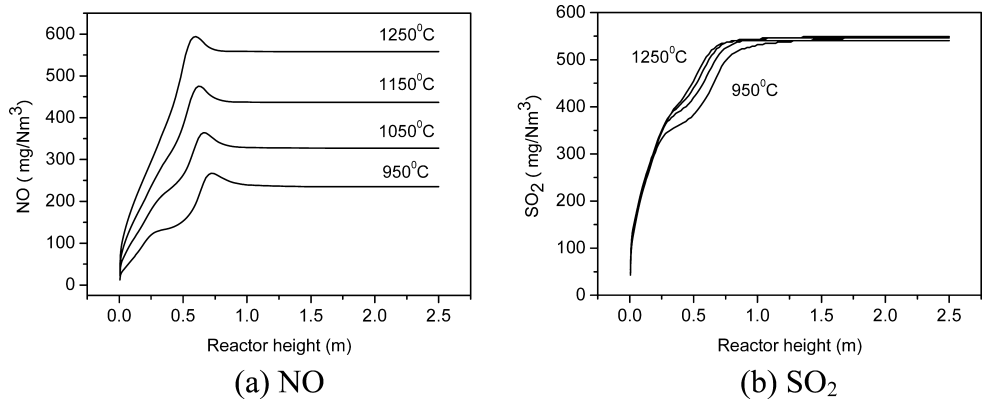

Figure 5. Predicted results of (a) NO and (b) SO_2 concentration distribution for pure Danish straw along the reactor height for various wall temperatures.

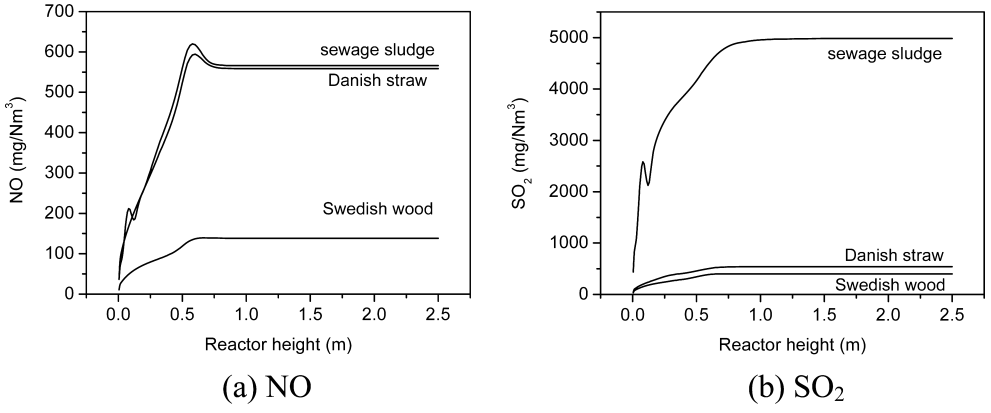

Figure 6. Predicted results of (a) NO and (b) SO_2 concentration distribution for Swedish wood, Danish straw, and sewage sludge along the reactor height at the temperature of 1250 °C.

biomass combustion or co-combustion of coal and biomass using AIOLOS, some work has been performed to validate its feasibility and rationality, such as refs 27 and 28.

3. PREDICTED RESULTS AND DISCUSSION

On the basis of the validation of the detailed modeling method, the effect of the combustion temperature on NO and SO_2 formation is analyzed, and the predicted results are shown in Figure 3 for the temperature range from 950 to 1250 °C. The simulation results of the same case published in ref 29 are slightly different, because it shows the values near the axis; however, in this paper, they are average values of the whole cross-section. Results indicate that the temperature significantly affects NO formation, and increasing the temperature obviously enhances the NO concentration, which coincides with the trend of measurement data.[26] In the range of the calculation, the final concentration level of SO_2 is not obviously affected by the temperature, and all of the concentration lines almost coincide with each other for different temperatures, with a higher temperature only leading to a little faster release process.

The combustion of three kinds of biomass fuels is also investigated. Biomass fuels are Swedish wood, Danish straw,

dx.doi.org/10.1021/ef201729r | Energy Fuels 2012, 26, 3117−3124

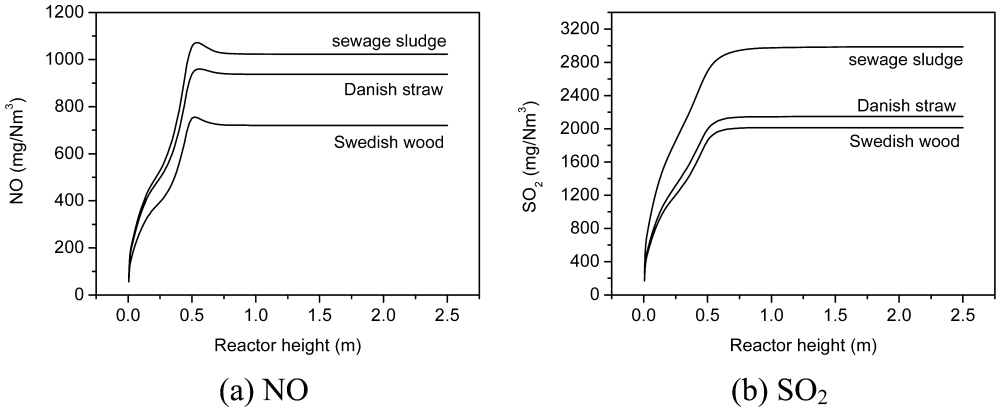

Figure 7. Predicted results of (a) NO and (b) SO_2 concentration distribution for co-combustion with Swedish wood, Danish straw, and sewage sludge along the reactor height (blending ratio, 25%; temperature, 1250 °C).

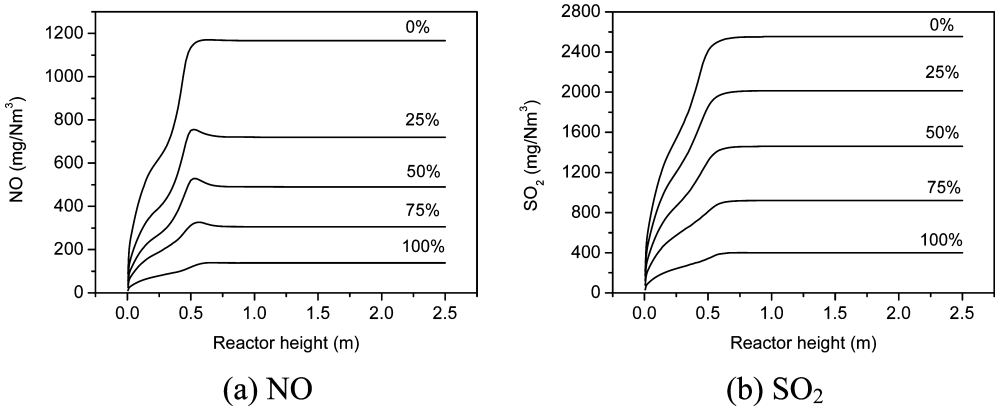

Figure 8. Modeling results of (a) NO and (b) SO_2 concentration distribution for co-combustion along the reactor height at the temperature of 1250 °C under different blending ratios of Swedish wood.

and sewage sludge, and the chemical analysis data of fuels are listed in Table 2. To coincide with the actual thermal power input, the simulation is based on the same heat release with 1 kg/h Göttelborn coal. Figure 4 shows the concentration profiles of NO and SO_2 emission during pure Swedish wood combustion. Although the trend of the curve is similar to those of coal combustion under various wall temperatures, the concentrations of the pollutant emissions are much lower than those of the coal obviously. This is because the wood has a very low content of nitrogen and sulfur and a high content of volatiles. Similar results can also be observed in Danish straw combustion, which is shown in Figure 5.

As mentioned above, although the combustion of biomass might reduce the pollutant emissions substantially, there are some differences in the chemical composition of biomass, which may influence NO and SO_2 emissions. Figure 6 shows NO and SO_2 concentration distributions during the combusting of the three different biomass fuels at 1250 °C. There are great differences of NO and SO_2 emissions for Swedish wood, Danish straw, and sewage sludge, which are caused by the different chemical composition shown in Table 2. The lower pollutant emissions of Swedish wood compared to those of Danish straw and sewage sludge are caused by its low content of nitrogen and sulfur. In addition, the high content of volatiles might result in an oxygen-poor atmosphere and limit the conversions of fuel N and fuel S to NO_x and SO_x. A low value of the lower heating value (LHV) can increase the demand of fuel, which will increase the source of fuel N and fuel S. This is a reason why the SO_2 emission is very high during sewage sludge combustion.

However, only burning pure biomass in a power plant might result in problems, such as a low LHV compared to coal and the deposition and corrosion possibility caused by alkali metals in biomass. To obtain low-pollutant emissions and good operation of the power plant, the co-combustion technology of coal and biomass is often applied. Because of the different composition of biomass fuels, co-combustion with biomass may influence pollutant emissions. In this paper, during the simulation of co-combustion of two fuels, the fuel with a larger mass flow is fed through carrying air inlet and the other is fed through carrying primary air inlet. The particle size distribution and kinetic parameters of each kind of fuel are given according to Table 1. Figure 7 shows the simulation results of co-combustion of Göttelborn coal and biomass fuels at the blending ratio of biomass at 25% and temperature of 1250 °C, where the blending ratio of biomass refers to the percentage of heat release for biomass and not the mass fraction. In comparison to the combustion of Göttelborn coal, the NO reductions of Swedish wood and Danish straw at the exit of the reactor are 38.30 and 19.67%, while the SO_2 reductions are 21.16 and 15.90%, respectively. For sewage sludge, the NO formation is reduced by 12.35%; however, the SO_2 formation is increased by 16.91%. The high SO_2 emission of sewage sludge is caused by the high content of sulfur and the low value of the LHV. Thereby, the biomass with low contents of nitrogen and

dx.doi.org/10.1021/ef201729r | Energy Fuels 2012, 26, 3117−3124

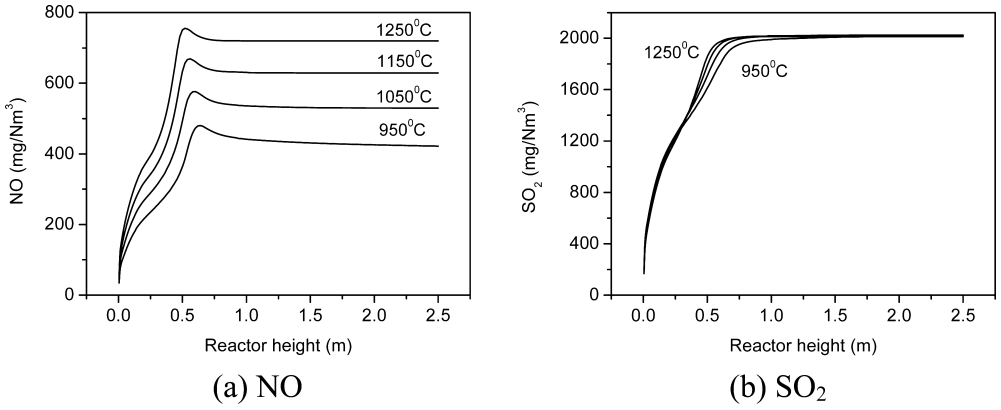

Figure 9. Modeling results of (a) NO and (b) SO_2 concentration distribution for co-combustion along the reactor height at the blending ratio of 25% of Swedish wood for various wall temperatures.

sulfur and a high volatile content and LHV is an ideal co-fired fuel to reduce NO and SO_2 emissions.

The results predicted above indicate that, among the three biomass fuels, Swedish wood is the best fuel to reduce pollutant emissions while co-combusting with coal. Figure 8 is the simulation results of co-combustion of Göttelborn coal and Swedish wood at the temperature of 1250 °C. Figure 9 shows the influence of the wall temperature on NO and SO_2 emissions at the blending ratio of 25%. These results indicate that co-combustion is affected by the temperature with the similar trend as the combustion of pure fuel. A low-temperature combustion can effectively reduce the formation of NO; however, the release process of SO_2 only slows, and its emission is not affected. The effect of co-combustion is proportional to the blending ratio of biomass; the higher the blending ratio of biomass, obviously the lower the NO and SO_2 emissions.

4. CONCLUSION

In the present work, a reduced reaction mechanism including N/S chemistry was developed on the basis of the detailed reaction mechanisms of "GADM98" and "GKDCB96" to investigate NO_x and SO_x formation in co-combustion of coal and biomass. The reduced mechanism with 15 species was integrated into a 3D combustion CFD program AIOLOS for simulation. The simulation results of coal combustion show good agreement with the experimental data, which provide a good validation for the simulation method and reduced mechanism.

The combustion of coal and biomass and co-combustion of coal and biomass were investigated through a large number of CFD simulations. The results indicate that the combustion of coal or biomass in EFR is affected by the temperature, and a lower temperature combustion can effectively reduce NO formation; however, the final concentration of SO_2 is almost not influenced by the temperature, with a higher temperature only leading to a little faster release process. The same influence can also be found while simulating co-combustion of coal and biomass fuels. Different biomass fuels can lead to different NO_x and SO_x emissions because of their chemical compositions. The biomass with low contents of nitrogen and sulfur and a high volatile content and LHV is an ideal co-fired fuel to reduce NO and SO_2 emissions. For co-combustion of coal and this kind of ideal biomass, a high blending ratio of biomass can lead to low NO and SO_2 emissions.

AUTHOR INFORMATION

Corresponding Author

*Telephone: +86-10-82544232. Fax: +86-10-62561284. E-mail: xlwei@imech.ac.cn.

ACKNOWLEDGMENTS

Financial support by the Alexander von Humboldt Foundation, the Chinese Natural Science Foundation (50776099 and 91130028), and the Knowledge Innovation Program of the Chinese Academy of Sciences (KGCX2-YW-321) is gratefully acknowledged. The authors also thank Professor P. Glarborg at the Technical University of Denmark (DTU) for his help on chemical mechanisms.

NOMENCLATURE

A_i = pre-exponential factor of the ith reaction
b = temperature exponent
E_i = activation energy of the ith reaction
K = total number of the species in a chemical reaction mechanism
k_f/k_r = forward/reverse reaction rate constant
LHV = lower heating value
n_{NO} = mole number of NO
q_i = rate of progress of the ith reaction
R = universal gas constant
S_e = available external surface area
$S_{k,i}$ = sensitivity coefficient of the kth species with respect to the ith reaction
T = temperature
X_k = mole fraction of the kth species
δ = predefined criterion
Δt = time of reaction stretch
ν'_{ki}/ν''_{ki} = stoichiometric coefficient of the kth species in the ith forward/reverse reaction
$\dot{\omega}_k^p/\dot{\omega}_k^d$ = production/destruction rate of the kth species

REFERENCES

(1) Hill, S. C.; Smoot, L. D. Modeling of nitrogen oxides formation and destruction in combustion systems. *Prog. Energy Combust. Sci.* **2000**, *26*, 417−458.

(2) Glarborg, P.; Jensen, A. D.; Johnsson, J. E. Fuel nitrogen conversion in solid fuel fired systems. *Prog. Energy Combust. Sci.* **2003**, *29* (2), 89−113.

(3) Miller, J. A.; Bowman, C. T. Mechanism and modeling of nitrogen chemistry in combustion. *Prog. Energy Combust. Sci.* **1989**, *15*, 287−338.

(4) Glarborg, P.; Alzueta, M. U.; Dam-Johansen, K.; Miller, J. A. Kinetic modeling of hydrocarbon/nitric oxide interactions in a flow reactor. *Combust. Flame* **1998**, *115*, 1−27.
(5) Bowman, C. T.; Hanson, R. K.; Davidson, D. F.; Gardiner, W. C. J.; Lissinsky, V.; Smith, G. P.; Golden, D. M.; Frenklach, M.; Goldenberg, M. *GRI-Mech Version 3.0*; GRI-Mech: Berkeley, CA, 2000; http://www.me.berkeley.edu/gri_mech/ (accessed July 2006).
(6) Xu, H.; Smoot, L. D.; Hill, S. C. A reduced kinetic model for NO_x reduction by advanced reburning. *Energy Fuels* **1998**, *12*, 1278−1289.
(7) Xu, H.; Smoot, L. D.; Hill, S. C. Computational model for NO_x reduction by advanced reburning. *Energy Fuels* **1999**, *13*, 411−420.
(8) Smooke, M. D. *Reduced Kinetic Mechanisms and Asymptotic Approximations for Methane−Air Flames*; Springer-Verlag: Heidelberg, Germany, 1991.
(9) Xu, H.; Smoot, L. D.; Tree, D. R.; Hill, S. C. Prediction of nitric oxide destruction by advanced reburning. *Energy Fuels* **2001**, *15* (3), 541−551.
(10) Han, X. H.; Rückert, F.; Schnell, U.; Hein, K. R. G.; Koger, S.; Bockhorn, H. Computational modelling of the NO_x-reduction process by hydrocarbon reburning with reduced kinetics. *Proceedings of Sixth International Conference on Technologies and Combustion for a Clean Environment*; Porto, Portugal, July 9−12, 2001.
(11) Han, X. H.; Wei, X. L.; Schnell, U.; Hein, K. R. G. Detailed modeling of hybrid reburn/SNCR processes for NO_x reduction in coal-fired furnaces. *Combust. Flame* **2003**, *132*, 374−386.
(12) Lv, Y.; Wang, Z. H.; Zhou, J. H.; Cen, K. F. Reduced mechanism for hybrid NO_x control process. *Energy Fuels* **2009**, *23* (12), 5920−5928.
(13) Rota, R.; Antos, D.; Zanoeto, E.; Morbidelli, M. Experiment and modeling analysis of the NO_xOUT process. *Chem. Eng. Sci.* **2002**, *57*, 27−38.
(14) Zabetta, E. G.; Hupa, M. *Scheme ÅA 2006-02-20*; Åbo Akademi University, Turku, Finland, 2006; http://www.abo.fi/tkf/cmc/research/r_schemes.html.
(15) Peters, N.; Rogg, B. *Reduced Kinetic Mechanisms for Applications in Combustion Systems*; Springer-Verlag: New York, 1993.
(16) Glarborg, P.; Kubel, D.; Dam-Johansen, K.; Chiang, H. M.; Bozzelli, J. W. Impact of SO_2 and NO on CO oxidation under post-flame conditions. *Int. J. Chem. Kinet.* **1996**, *28* (10), 773−790.
(17) Lutz, A. E.; Kee, R. J.; Miller, J. A. *SENKIN: A Fortran Program for Predicting Homogeneous Gas Phase Chemical Kinetics with Sensitivity Analysis*; Sandia National Laboratories: Albuquerque, NM, 1988; Report SAND87-8248.
(18) Han, X. H.; Ruckert, F; Schnell, U.; Hein, K. R. G.; Koger, S.; Bockhorn, H. Computational modeling of NO_x reburning by hydrocarbons in a coal furnace with reduced kinetics. *Combust. Sci. Technol.* **2003**, *175*, 523−544.
(19) Schnell, U. Numerical modeling of solid fuel combustion processes using advanced CFD-based simulation tools. *Int. J. Prog. Comput. Fluid Dyn.* **2001**, *1* (4), 208−218.
(20) Magnussen, B. F.; Hjertager, B. H. On mathematical modeling of turbulent combustion with special emphasis on soot formation and combustion. *Proc. Combust. Inst.* **1976**, *16*, 719−217.
(21) Gran, I. R.; Magnussen, B. F. A numerical study of a bluff-body stabilized diffusion flame. Part 1. Influence of turbulence modelling and boundary conditions. *Combust. Sci. Technol.* **1996**, *119*, 171−190.
(22) Gran, I. R.; Magnussen, B. F. A numerical study of a bluff-body stabilized diffusion flame. Part 2. Influence of combustion modelling and finite-rate chemistry. *Combust. Sci. Technol.* **1996**, *119*, 191−217.
(23) Magel, H. C.; Schnell, U.; Hein, K. R. G. Simulation of detailed chemistry in a turbulent combustor flow. *Proc. Combust. Inst.* **1996**, *26*, 67−74.
(24) Förtsch, D.; Kluger, F.; Schnell, U.; Spliethoff, H.; Hein, K. R. G. A kinetic model for the prediction of NO emissions from staged combustion of pulverized coal. *Proc. Combust. Inst.* **1998**, *27*, 3037−3044.
(25) Solomon, P. R.; Fletcher, T. H.; Pugmire, R. J. Progress in coal pyrolysis. *Fuel* **1993**, *72*, 587−597.
(26) Wei, X. L.; Han, X. H.; Schnell, U.; Maier, J.; Worner, H.; Hein, K. R. G. The effect of HCl and SO_2 on NO_x formation in coal flames. *Energy Fuels* **2003**, *17*, 1392−1398.
(27) Heikkinen, J. M.; Venneker, B. C. H.; di Nola, G.; de Jong, W.; Spliethoff, H. CFD simulation and experimental validation of co-combustion of chicken litter and MBM with pulverized coal in a flow reactor. *Fuel Process. Technol.* **2008**, *89*, 874−889.
(28) Kurz, D.; Schnell, U.; Scheffknecht, G. CFD simulation of wood chip combustion on a grate using an Euler−Euler approach. *Combust. Theory Modell.* **2011**, 1−23.
(29) Wei, X. L.; Han, X. H.; Schnell, U.; Scheffknecht, G.; Risio, B. Modeling of the NO_x and SO_x formation in pulverized coal combustion with detailed reaction mechanism. *Chin. J. Theor. Appl. Mech.* **2008**, *40*, 760−768 (in Chinese).